Joint Active and Passive Beamforming for IRS-Assisted Radar

Fangzhou Wang D, Student Member, IEEE, Hongbin Li D, Fellow, IEEE, and Jun Fang, Senior Member, IEEE

Abstract—Intelligent reflecting surface (IRS) is a promising technology being considered for future wireless communications due to its ability to control signal propagation. This paper considers the joint active and passive beamforming problem for an IRS-assisted radar, where multiple IRSs are employed to assist the surveillance of multiple targets in cluttered environments. Specifically, we aim to maximize the minimum target illumination power at multiple target locations by jointly optimizing the active beamformer at the radar transmitter and the passive phase-shift matrices at the IRSs, subject to an upperbound on the clutter power at each clutter scatterer. The resulting optimization problem is nonconvex and solved with a sequential optimization procedure along with semidefinite relaxation (SDR). Simulation results show that additional line-of-sight (LOS) paths created by IRSs can substantially improve the radar robustness against target blockage.

Index Terms—Intelligent reflecting surface, radar, non-line of sight, beamforming, optimization.

I. INTRODUCTION

N RECENT years, intelligent reflecting surface (IRS) has attracted significant attention for wireless communication [1]–[5]. IRS is a planar array consisting of dozens of low-cost passive elements, which are capable of changing the phase and polarization of the impinging signals, thereby collaboratively achieving controllable signal reflection. Unlike existing approaches that modify the wireless link at the transmitter/receiver, IRS can be employed to realize programmable wireless channels between them, thus offering additional degrees of freedom for system design [6].

Although the use of IRS was firstly proposed for communication purposes, it has recently gained significant attention within the radar research community. One group of works examined the integration of IRS for cooperative radar and communication systems [7]–[10]. Specifically, the IRS was used to mitigate multi-user interference by joint waveform design and passive beamforming for a dual-functional radar-communication (DFRC) system [7], and respectively,

Manuscript received November 3, 2021; revised December 2, 2021; accepted December 7, 2021. Date of publication December 13, 2021; date of current version January 28, 2022. This work was supported by the National Science Foundation under Grant ECCS-1923739. The associate editor coordinating the reviewof this manuscript and approving it for publication was Dr. Jens Ahrens. (Corresponding author: Hongbin Li.)

Fangzhou Wang and Hongbin Li are with the Department of Electrical and Computer Engineering, Stevens Institute of Technology, Hoboken, NJ 07030 USA (e-mail: fwang11@stevens.edu; hli@stevens.edu).

Jun Fang is with the National Key Laboratory of Science and Technology on Communications, University of Electronic Science and Technology of China, Chengdu 611731, China (e-mail: junfang@uestc.edu.cn).

Digital Object Identifier 10.1109/LSP.2021.3134899

spectrum sharing between multi-input multi-output (MIMO) radar and multi-user multi-input single-output communication systems [8]. In [9], the IRS was utilized in a DFRC system to improve target detection in environments with severe path loss, while [10] proposed to adaptively partition the IRS to enhance the radar sensing and communication capabilities of a millimeter-wave DFRC system. Another group of recent works, e.g., [11]–[14], focused on exploiting IRS to enhance the sensing performance in radar. Specifically, the phase-shift matrix of the IRS was optimized for colocated MIMO radar [11], and respectively, distributed MIMO radar [12] to improve the estimation and detection performance. Target detection was also considered in cases when the radar is aided by a single IRS [13] or multiple IRSs [14].

Detection and localization of moving targets such as pedestrians and vehicles in urban environments is a challenging radar problem [15]. Conventional radar applications usually assume that targets are in line of sight (LOS) with the radar. In practice, the LOS path may be blocked by buildings in urban environments. One way to handle the problem is to use a radar network. For example, [16] proposed a distributed radar to create continuous coverage in urbanized environments. A different and more economic way is to employ the IRS technology. Along this direction, [17] analyzed the effect of IRS on radar equations for surveillance in non-line of sight (N-LOS) scenarios. In [18], a single IRS is employed to illuminate a mobile user in the context of localization when the LOS between the base station and the user is not available.

In this paper, we consider a radar system assisted by multiple IRSs for target surveillance in a cluttered environment, where the LOS paths from the radar transmitter to prospective targets may be blocked by clutter scatterers. Target blocking is frequently encountered in an indoor setting when a single radar TX is unable to cover the entire surveillance area. A joint beamforming design is formulated, which maximizes the minimum target illumination power of multiple targets with respect to the active transmit beamformer and the passive phase-shift matrices of the IRSs, while imposing a total transmit power constraint as well as an upperbound on the tolerable clutter power at each clutter scatterer. The proposed design results in a nonconvex constrained optimization problem. We propose a sequential optimization procedure which employs semidefinite relaxation (SDR) to find the active and passive beamformers in an iterative manner. Simulation results show that our proposed joint design for the IRS-assisted radar can significantly decrease the probability of blockage for targets over conventional radar system that is not equipped with an IRS, or the IRS-assisted radar system that employs only the active or passive design.

1070-9908 © 2021 IEEE. Personal use is permitted, but republication/redistribution requires IEEE permission. See https://www.ieee.org/publications/rights/index.html for more information.

II. PROBLEM FORMULATION

Consider an IRS-assisted radar system, where a multiantenna transmitter tracks multiple targets with the help of multiple IRSs. The transmitter (TX) is equipped with M antenna elements. A beamforming vector $\mathbf{t} \in \hat{\mathbb{C}}^{M \times 1}$ is designed to transmit a common waveform. A total of K IRSs, each comprising N reflecting elements, are deployed to assist the illumination of multiple prospective targets. Each element on the IRS combines the impinging signals with a certain phase shift [19]. By denoting $\theta_{k,n} \in [0, 2\pi]$ as the phase shift associated with the n-th element of the k-th IRS, the diagonal matrix accounting for the phase response of the k-th IRS can be expressed as $\Theta_k \triangleq \text{diag}(e^{j\theta_{k,1}}, \dots, e^{j\theta_{k,N}})$. Suppose there are Ltargets and Q clutter scatterers located in the surveillance area. Then, the signals from the radar TX and K IRSs superimposed at the ℓ -th target are $(\mathbf{h}_{t,\ell}^T + \sum_{k=1}^K \mathbf{h}_{i,k,\ell}^T \mathbf{\Theta}_k^H \mathbf{D}_k) \mathbf{t}$, and, likewise, the signals from the TX and IRSs superimposed at the q-th clutter scatterer are $(\mathbf{g}_{\mathsf{t},q}^T + \sum_{k=1}^K \mathbf{g}_{\mathsf{i},k,q}^T \mathbf{\Theta}_k^H \mathbf{D}_k)\mathbf{t}$, where $\mathbf{h}_{\mathsf{t},\ell} \in \mathbb{C}^{M \times 1}$ denotes the channel between the TX and the

- $\mathbf{h}_{\mathrm{t},\ell} \in \mathbb{C}^{M \times 1}$ denotes the channel between the TX and the ℓ -th target, $\mathbf{h}_{\mathrm{i},k,\ell} \in \mathbb{C}^{N \times 1}$ the channel between the k-th IRS and the ℓ -th target, and $\mathbf{D}_k \in \mathbb{C}^{N \times M}$ the channel between the TX and the k-th IRS.
- between the TX and the k-th IRS.

 $\mathbf{g}_{t,q} \in \mathbb{C}^{M \times 1}$ and $\mathbf{g}_{i,k,q} \in \mathbb{C}^{N \times 1}$ denote the channel from the TX, and respectively, the k-th IRS to the q-th clutter scatterer.

The problem of interest is to jointly design the TX beamformer t and IRS phase-shift matrices $\{\Theta_k\}$ by maximizing the minimum illumination power at the target locations, subject to a total radar transmit power constraint as well as an upperbound on the clutter power for each clutter scatterer. Specifically, our joint design can be formulated as:

$$\max_{\mathbf{t}, \{\boldsymbol{\Theta}_k\}} \min_{\ell=1,\dots,L} \left| \left(\mathbf{h}_{t,\ell}^T + \sum_{k=1}^K \mathbf{h}_{i,k,\ell}^T \boldsymbol{\Theta}_k^H \mathbf{D}_k \right) \mathbf{t} \right|^2$$
 (1a)

s.t.
$$\mathbf{t}^H \mathbf{t} \le \kappa$$
, $\left| \left(\mathbf{g}_{\mathbf{t},q}^T + \sum_{k=1}^K \mathbf{g}_{\mathbf{i},k,q}^T \mathbf{\Theta}_k^H \mathbf{D}_k \right) \mathbf{t} \right|^2 \le \eta_q, \, \forall q,$

$$\tag{1b}$$

$$\Theta_k = \operatorname{diag}\left(e^{j\theta_{k,1}}, \dots, e^{j\theta_{k,N}}\right), \forall k, \tag{1c}$$

where κ denotes the maximum transmit power and η_q is the upperbound of the tolerable clutter power for the q-th clutter scatterer. In this paper, since our goal is to illuminate the target, the exact channel information is not needed and only the LOS channel is required. According to the standard radar equation [20], the channel can be modeled as a function of the target position. Here, we assume that the target position is known since it can either be estimated from the previous tracking or be a pre-specified illumination aim, i.e., radar sequentially scans potential surveillance areas to determine whether the area/location of interest has a target or not.

III. PROPOSED SOLUTION

In this section, a solution to the joint design is presented. Note that problem (1) is nonconvex with respect to (w.r.t.) the design variables. Our approach is to decompose the original problem into two simpler subproblems by fixing either t or

 Θ_k and solving them sequentially and iteratively, which leads to an alternating optimization procedure. Specifically, during the (j+1)-st iteration, problem (1) can be simplified to a subproblem w.r.t. only t by fixing Θ_k as $\Theta_k^{(j)}$:

$$\max_{\mathbf{t}} \min_{\ell=1,\dots,L} \left| \left(\mathbf{h}_{\mathsf{t},\ell}^T + \sum_{k=1}^K \mathbf{h}_{\mathsf{i},k,\ell}^T \left(\boldsymbol{\Theta}_k^{(j)} \right)^H \mathbf{D}_k \right) \mathbf{t} \right|^2 \quad (2a)$$

$$s.t. t^H t < \kappa, \tag{2b}$$

$$\left| \left(\mathbf{g}_{\mathsf{t},q}^T + \sum_{k=1}^K \mathbf{g}_{\mathsf{i},k,q}^T \left(\mathbf{\Theta}_k^{(j)} \right)^H \mathbf{D}_k \right) \mathbf{t} \right|^2 \le \eta_q, \, \forall q. \, (2c)$$

This is a nonconvex quadratically constrained quadratic programming (QCQP) problem and can be solved by using the semidefinite relaxation (SDR) technique. Specifically, by letting $\mathbf{T} = \mathbf{t}\mathbf{t}^H$ and dropping the rank-one constraint, problem (2) can be rewritten as

$$\max_{\mathbf{T}} \min_{\ell=1,\dots,L} \operatorname{tr}(\mathbf{A}_{\ell}\mathbf{T})$$
 (3a)

s.t.
$$\operatorname{tr}(\mathbf{T}) \le \kappa$$
, $\operatorname{tr}(\mathbf{B}_q \mathbf{T}) \le \eta_q$, $\forall q$, (3b)

where $\mathbf{A}_{\ell} = \mathbf{a}_{\ell} \mathbf{a}_{\ell}^{H}$, $\mathbf{a}_{\ell}^{H} = \mathbf{h}_{t,\ell}^{T} + \sum_{k=1}^{K} \mathbf{h}_{i,k,\ell}^{T} (\boldsymbol{\Theta}_{k}^{(j)})^{H} \mathbf{D}_{k}$, $\mathbf{B}_{q} = \mathbf{b}_{q} \mathbf{b}_{q}^{H}$, and $\mathbf{b}_{q}^{H} = \mathbf{g}_{t,q}^{T} + \sum_{k=1}^{K} \mathbf{g}_{i,k,q}^{T} (\boldsymbol{\Theta}_{k}^{(j)})^{H} \mathbf{D}_{k}$. Note that problem (3) is convex and can be solved with numerical solvers, e.g., CVX [21].

The SDR solution $\mathbf{T}^{(j+1)}$ to (3) needs to be converted into a feasible solution $\mathbf{t}^{(j+1)}$ to (2), which can be achieved through a randomization approach [22], [23]. Specifically, we can use $\mathbf{T}^{(j+1)}$ to generate I Gaussian random vectors, i.e., $\boldsymbol{\xi}_i \sim \mathcal{CN}(\mathbf{0},\mathbf{T}^{(j+1)}), i=1,\ldots,I$, to conduct the randomization procedure. Note that the random vectors $\boldsymbol{\xi}_i$ are not always feasible for (2), but we can apply a scaling to turn them into feasible solutions. Specifically, $\boldsymbol{\xi}_i$ can be normalized w.r.t. the largest value of $\{\boldsymbol{\xi}_i^H \boldsymbol{\xi}_i/\kappa, \boldsymbol{\xi}_i^H \mathbf{B}_1 \boldsymbol{\xi}_i/\eta_1, \cdots, \boldsymbol{\xi}_i^H \mathbf{B}_Q \boldsymbol{\xi}_i/\eta_Q\}$:

$$\widetilde{\boldsymbol{\xi}}_{i} = \frac{\boldsymbol{\xi}_{i}}{\sqrt{\max\left\{\boldsymbol{\xi}_{i}^{H}\boldsymbol{\xi}_{i}/\kappa, \, \boldsymbol{\xi}_{i}^{H}\mathbf{B}_{1}\boldsymbol{\xi}_{i}/\eta_{1}, \, \cdots, \, \boldsymbol{\xi}_{i}^{H}\mathbf{B}_{Q}\boldsymbol{\xi}_{i}/\eta_{Q}\right\}}}.$$
(4)

After randomization, a feasible rank-one solution is obtained as $\mathbf{t}^{(j+1)} = \arg\max_{\widetilde{\boldsymbol{\xi}}_i} \min_{\ell=1,\dots,L} \ \widetilde{\boldsymbol{\xi}}_i^H \mathbf{A}_\ell \widetilde{\boldsymbol{\xi}}_i.$

Next, we find Θ_k by fixing t to the value obtained from the latest updates, $\mathbf{t}^{(j+1)}$, in which case the optimization problem (1) becomes

$$\max_{\{\boldsymbol{\Theta}_k\}} \min_{\ell=1,\dots,L} \left| \left(\mathbf{h}_{t,\ell}^T + \sum_{k=1}^K \mathbf{h}_{i,k,\ell}^T \boldsymbol{\Theta}_k^H \mathbf{D}_k \right) \mathbf{t}^{(j+1)} \right|^2$$
 (5a)

s.t.
$$\left\| \left(\mathbf{g}_{\mathsf{t},q}^T + \sum_{k=1}^K \mathbf{g}_{\mathsf{i},k,q}^T \mathbf{\Theta}_k^H \mathbf{D}_k \right) \mathbf{t}^{(j+1)} \right\|^2 \le \eta_q, \ \forall q, \ \ (5b)$$

$$\Theta_k = \operatorname{diag}\left(e^{j\theta_{k,1}}, \dots, e^{j\theta_{k,N}}\right), \forall k.$$
 (5c)

Let $\widetilde{\mathbf{h}}_{\mathbf{i},k,\ell} = \mathbf{h}_{\mathbf{i},k,\ell} \circ (\mathbf{D}_k \mathbf{t}^{(j+1)}), \quad \widetilde{\mathbf{g}}_{\mathbf{i},k,q} = \mathbf{g}_{\mathbf{i},k,q} \circ (\mathbf{D}_k \mathbf{t}^{(j+1)}), \quad \boldsymbol{\theta}_k = [e^{j\theta_{k,1}},\dots,e^{j\theta_{k,N}}]^T, \quad \text{where} \quad \circ \quad \text{denotes}$ the Hadamard (elementwise) product. Then, problem (5) can

be rewritten as

$$\max_{\{\boldsymbol{\theta}_k\}} \min_{\ell=1,\dots,L} \left| \mathbf{h}_{t,\ell}^T \mathbf{t}^{(j+1)} + \sum_{k=1}^K \boldsymbol{\theta}_k^H \widetilde{\mathbf{h}}_{i,k,\ell} \right|^2$$
(6a)

s.t.
$$\left| \mathbf{g}_{\mathsf{t},q}^T \mathbf{t}^{(j+1)} + \sum_{k=1}^K \boldsymbol{\theta}_k^H \widetilde{\mathbf{g}}_{\mathsf{i},k,q} \right|^2 \le \eta_q, \, \forall q,$$
 (6b)

$$|\boldsymbol{\theta}_k(n)| = 1, \, \forall k, \, \forall n.$$
 (6c)

To write the above cost function and constraints in a more compact form, we define $\mathbf{h}_\ell = [\widetilde{\mathbf{h}}_{i,1,\ell}^T, \dots, \widetilde{\mathbf{h}}_{i,K,\ell}^T]^T, \mathbf{g}_q = [\widetilde{\mathbf{g}}_{i,1,q}^T, \dots, \widetilde{\mathbf{g}}_{i,K,q}^T]^T$, and $\boldsymbol{\theta} = [\boldsymbol{\theta}_1^T, \dots, \boldsymbol{\theta}_K^T]^T$. Hence, (6) can be simplified as

$$\max_{\boldsymbol{\theta}} \min_{\ell=1,\dots,L} \left| a_{\ell} + \boldsymbol{\theta}^{H} \mathbf{h}_{\ell} \right|^{2}$$
 (7a)

s.t.
$$\left|b_q + \boldsymbol{\theta}^H \mathbf{g}_q\right|^2 \le \eta_q, \, \forall q,,$$
 (7b)

$$|\theta(l)| = 1, l = 1, \dots, NK,$$
 (7c)

where $a_\ell = \mathbf{h}_{\mathsf{t},\ell}^T \mathbf{t}^{(j+1)}$ and $b_q = \mathbf{g}_{\mathsf{t},q}^T \mathbf{t}^{(j+1)}$. Note that the above problem is nonconvex because of the unit modulus constraint (7c). However, by observing that the objective function and constraint (7b) can be transformed into quadratic forms, we can apply the SDR technique to approximately solve (7) efficiently.

Specifically, an auxiliary variable t can be introduced to convert the non-homogeneous QCQP problem (7) into a homogeneous one:

$$\max_{\bar{\boldsymbol{\theta}}} \min_{\ell=1,\dots,L} \bar{\boldsymbol{\theta}}^H \mathbf{H}_{\ell} \bar{\boldsymbol{\theta}} + |a_{\ell}|^2$$
 (8a)

s.t.
$$\bar{\boldsymbol{\theta}}^H \mathbf{G}_q \bar{\boldsymbol{\theta}} + |b_q|^2 \le \eta_q, \, \forall q,$$
 (8b)

$$|\bar{\theta}(l)| = 1, l = 1, \dots, NK + 1,$$
 (8c)

where $\bar{\boldsymbol{\theta}} = [\boldsymbol{\theta}^T, t]^T$ and

$$\mathbf{H}_{\ell} = \begin{bmatrix} \mathbf{h}_{\ell} \mathbf{h}_{\ell}^{H} & \mathbf{h}_{\ell} a_{\ell}^{*} \\ \mathbf{h}_{\ell}^{H} a_{\ell} & 0 \end{bmatrix}, \mathbf{G}_{q} = \begin{bmatrix} \mathbf{g}_{q} \mathbf{g}_{q}^{H} & \mathbf{g}_{q} b_{q}^{*} \\ \mathbf{g}_{q}^{H} b_{q} & 0 \end{bmatrix}. \tag{9}$$

Similarly, problem (8) can be solved through the SDR technique, i.e., define $\Theta = \bar{\theta}\bar{\theta}^H$ and drop the rank-one constraint. Then, problem (8) can be rewritten as

$$\max_{\boldsymbol{\Theta}} \min_{\ell=1,\dots,L} \operatorname{tr}(\boldsymbol{\Theta} \mathbf{H}_{\ell}) + |a_{\ell}|^2 \tag{10a}$$

s.t. tr
$$(\Theta \mathbf{G}_a) + |b_a|^2 < \eta_a, \forall q,$$
 (10b)

$$|\Theta(l,l)| = 1, l = 1, \dots, NK + 1,$$
 (10c)

which is a convex problem and can be solved by CVX. A similar randomization procedure as in (4) can be employed to obtain a solution $\boldsymbol{\theta}^{(j+1)}$ from $\boldsymbol{\Theta}^{(j+1)}$ except that the scaling becomes

$$\widetilde{\boldsymbol{\xi}}_i = \frac{\boldsymbol{\xi}_i}{\sqrt{\max_{q=1,\dots,Q} \boldsymbol{\xi}_i^H \mathbf{G}_q \boldsymbol{\xi}_i / (\eta_q - |b_q|^2)}}, \quad (11)$$

which makes $\widetilde{\boldsymbol{\xi}}_i$ to satisfy the constraint (8b). In addition, $\widetilde{\boldsymbol{\xi}}_i$ should meet the unit modulus constraint (8c), which means

Algorithm 1: Proposed Solution to (1).

Input: $\mathbf{h}_{t,\ell}$, $\mathbf{h}_{i,k,\ell}$, $\mathbf{h}_{t,\ell}$, $\mathbf{h}_{i,k,\ell}$, \mathbf{D}_k , κ , η_q , and tolerance ϵ . **Output:** Transmit beamformer \mathbf{t} and phase shift matrices Θ_k .

Initialization: Initialize $\Theta_k^{(0)}$ and j=0. repeat

- 1: Fix $\Theta_k^{(j)}$. Use (3) and randomization (4) to obtain $\mathbf{t}^{(j+1)}$.
- 2: Fix $\mathbf{t}^{(j+1)}$. Use (10) along with randomization (11) to find $\boldsymbol{\theta}^{(j+1)}$.
- 3: Use $\theta^{(j+1)}$ to formulate $\Theta_k^{(j+1)}$.
- 4: Set j = j + 1.

untilconvergence.

return $\mathbf{t} = \mathbf{t}^{(j+1)}$ and $\mathbf{\Theta}_k = \mathbf{\Theta}_k^{(j+1)}$.

the final solution can be recovered by $\hat{\boldsymbol{\xi}}_i = e^{j\arg(\frac{\boldsymbol{\xi}_i}{\hat{\boldsymbol{\xi}}_i(NK+1)})}$, where $\widetilde{\boldsymbol{\xi}}_i(NK+1)$ denotes the (NK+1)-st element of $\widetilde{\boldsymbol{\xi}}_i$. Then, a feasible rank-one solution is obtained as $\bar{\boldsymbol{\theta}}^{(j+1)} = \arg\max_{\hat{\boldsymbol{\xi}}_i} \min_{\ell=1,\dots,L} \hat{\boldsymbol{\xi}}_i^H \mathbf{H}_\ell \hat{\boldsymbol{\xi}}_i + |a_\ell|^2$. The alternating process is repeated until the improvement of the objective function between two iterations is smaller than a tolerance ϵ . Algorithm 1 summarizes our proposed alternating algorithm for the joint design problem.

The computational complexity of the proposed solution is mainly determined by the iteration number J and the SDR randomization trials I. Specifically, inside each iteration, two convex problems are solved with a total complexity of $\mathcal{O}(2JN^{3.5})$ by using an interior-point method [24]. In addition, for each iteration, two randomization procedures are required with a computational complexity of $\mathcal{O}(IM^2)$ for (4), and respectively, $\mathcal{O}(I(NK+1)^2)$ for (11). Thus, the overall complexity of the proposed approach is $\mathcal{O}(2JN^{3.5}) + \mathcal{O}(JIM^2) + \mathcal{O}(JI(NK+1)^2)$. Numerical results show that **Algorithm 1** usually converges within 20 iterations and a sufficiently large number of randomization, e.g., I=5000, is required to yield a good solution. Although the overall complexity is polynomial, more computing resource is required for large N and real-time updates of designs.

IV. NUMERICAL RESULTS

In this section, numerical results are provided to demonstrate the performance of the proposed scheme. In the simulation, there are one radar TX and two IRSs, where the TX is a uniform linear array (ULA) with M=64 antennas while each IRS consists of N=100 reflecting elements. The channel vectors $\mathbf{h}_{t,\ell}$, $\mathbf{h}_{i,k,\ell}$, $\mathbf{g}_{t,\ell}$, and $\mathbf{g}_{i,k,\ell}$ are generated as [25] (here we take $\mathbf{h}_{t,\ell}$ as an example and the other channel vectors are similarly generated): $\mathbf{h}_{t,\ell} = \sqrt{M}\alpha_{t,\ell}\gamma\mathbf{h}(\phi_{t,\ell})$, where $\alpha_{t,\ell}$ is a complex coefficient accounting for the channel gain from the TX to the ℓ -th target, $\phi_{t,\ell}$ is the look direction of the corresponding target, $\mathbf{h} \in \mathbb{C}^{M \times 1}$ denotes the normalized steering vector, and $\gamma \in \{1,0\}$ is a binary variable to specify if this path is blocked or not (more discussion on this in the next paragraph). The channel coefficient is generated as [26]: $\alpha_{t,\ell} \sim \mathcal{CN}(0, 10^{-0.1\lambda})$, where $\lambda = a + 10b \log_{10}(d) + \xi$, a = 64, b = 2, and $\xi \sim \mathcal{N}(0, \sigma^2)$

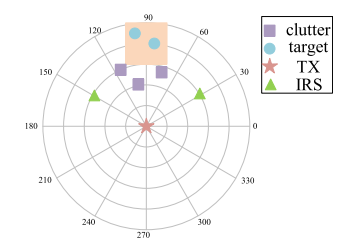


Fig. 1. Simulation setup.

with $\sigma=5.8 \mathrm{dB}$. Note that d represents the distance between the TX and the target. These parameters are selected according to the real-world LOS channel measurements [26]. In addition, the channel matrix between the transmitter and the k-th IRS is characterized by $\mathbf{D}_k = \sqrt{M_t N} \alpha_k \mathbf{d}_{\mathrm{r},k} \mathbf{d}_{\mathrm{t},k}^H$, where α_k is the complex gain and can be similarly generated as $\alpha_{\mathrm{t},\ell}$, $\mathbf{d}_{\mathrm{r},k}$ and $\mathbf{d}_{\mathrm{t},k}$ are the normalized steering vectors.

Fig. 1 shows simulation configuration, where the (x,y)-coordinates of the TX are (0,0) and those of the two IRSs are $(-130\,\mathrm{m},75\,\mathrm{m})$ and $(130\,\mathrm{m},75\,\mathrm{m})$. The locations of the targets are randomly distributed within a square box specified by $x \in [-75\,\mathrm{m}\,75\,\mathrm{m}]$ and $y \in [150\,\mathrm{m}\,250\,\mathrm{m}]$. To simulate the effect of blockage, we use the 3 dB beamwidth of the TX [20]. Specifically, if the TX beam simultaneously covers multiple objects (targets or clutter scatterers) within the 3 dB beamwidth, then the near object will block the far object, which is simulated by setting $\gamma=0$ for the far path. Other system parameters are set as follows: $\epsilon=10^{-3},~\eta_q=0.5~\mu\mathrm{W},~\forall q,~I=5000$. All results are averaged over 100 random channel realizations (also the randomization of the target locations).

In the simulation, the performance of the following four design approaches are included: The joint (exact), passive (exact), and active (exact) are the proposed joint active and passive beamforming (design t and Θ_k), the passive-only beamforming (design Θ_k by fixing t so that the TX illuminates toward the first IRS), and respectively, the active-only beamforming (design t by fixing Θ_k as identity matrix) for the IRS-assisted radar system; no IRS (exact) is the conventional radar system that has the TX but no IRS (design t). Note that in practice the exact channel information is not available and estimated channels have to be employed for the design. To demonstrate the impact of channel estimation errors, we also include results obtained by using estimated channels, which contain an estimation error in an average of 5% for the channel amplitude coefficient $\alpha_{t,\ell}$ and an estimation error in an average of $\pm 3^{\circ}$ (3 dB beamwidth) for the looking angle $\phi_{t,\ell}$ (we take $\mathbf{h}_{t,\ell}$ as an example and the errors in the other channel vectors are similar). The results of using estimated channels are denoted as estimate instead of exact.

Fig. 2 depicts the performance for the four design approaches versus the total transmit power κ when Q=3 and the clutter scatterers locate at $(-75\,\mathrm{m},125\,\mathrm{m}),~(0,125\,\mathrm{m}),$ and $(75\,\mathrm{m},125\,\mathrm{m}),~\mathrm{respectively}.$ In Fig. 2(a), which shows the minimum target illumination power, it is seen that the three IRS-assisted radars outperform the conventional radar system because additional LOS paths are created by the IRSs to illuminate the targets and thus substantially improve the radar's robustness against blockage. This can also been seen in Fig. 2(b) where the probability of blockage (Pb) is plotted, where blockage occurs when the target illumination power is

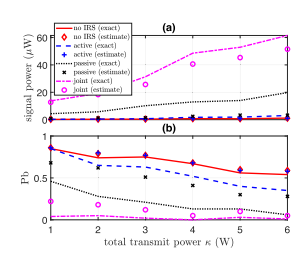


Fig. 2. Performance versus κ when Q=3: (a) minimum target illumination power, (b) probability of target blockage.

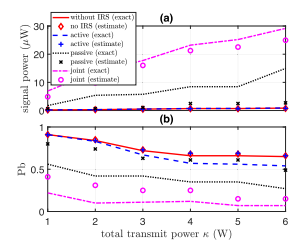


Fig. 3. Performance versus κ when Q=9: (a) minimum target illumination power, (b) probability of target blockage.

sufficiently small. In our simulation, the blockage power level is set to $0.5~\mu W$. It is observed that although also assisted by IRSs, the active- and passive-only designs are significantly less effective than the joint design.

Fig. 3 depicts the results for a more densely cluttered environment with Q=9 clutter scatterers, where the clutter scatterer locations are $(-75\,\mathrm{m},100\,\mathrm{m}),\,(0,100\,\mathrm{m}),\,(75\,\mathrm{m},100\,\mathrm{m}),\,(-75\,\mathrm{m},125\,\mathrm{m}),\,(0,125\,\mathrm{m}),\,(75\,\mathrm{m},125\,\mathrm{m}),\,(-75\,\mathrm{m},150\,\mathrm{m}),\,(0,150\,\mathrm{m}),\,\mathrm{and}\,(75\,\mathrm{m},150\,\mathrm{m}).$ Similar behaviors among the four designs can be observed except that the performance of all decreases. This is because more clutters means that the targets have a higher possibility of being blocked, which reduces the propagation paths. However, the joint design for the IRS-assisted system still outperforms the other designs.

Fig. 2 and Fig. 3 show that the performance of all designs degrades when estimated channels are employed for the design. However, even with estimated channels, our proposed joint design still provides significant performance gains over the other designs in terms of both illumination power and blocking probability.

V. CONCLUSION

We proposed an approach to reducing the target blockage in radar systems in cluttered environments by leveraging passive IRSs. Under a total transmit power constraint as well as an upperbound on the tolerable clutter power at each clutter scatterer, the active transmit beamforming vector at the radar and the passive phase-shift matrices at the IRSs were jointly optimized to maximize the minimum target illumination power at multiple target locations. The resulting nonconvex problem was solved by applying the alternating optimization and SDR techniques. Simulation results have shown that the IRS-assisted radar system is more robust against target blockage over conventional radar system.

REFERENCES

- [1] E. Basar, M. Di Renzo, J. De Rosny, M. Debbah, M.-S. Alouini, and R. Zhang, "Wireless communications through reconfigurable intelligent surfaces," *IEEE Access*, vol. 7, pp. 116753–116773, 2019.
- [2] Q. Wu and R. Zhang, "Towards smart and reconfigurable environment: Intelligent reflecting surface aided wireless network," *IEEE Commun. Mag.*, vol. 58, no. 1, pp. 106–112, Jan. 2020.
- [3] C. Pan et al., "Reconfigurable intelligent surfaces for 6G systems: Principles, applications, and research directions," *IEEE Commun. Mag.*, vol. 59, no. 6, pp. 14–20, Jun. 2021.
- [4] P. Wang, J. Fang, H. Duan, and H. Li, "Compressed channel estimation for intelligent reflecting surface-assisted millimeter wave systems," *IEEE Signal Process. Lett.*, vol. 27, pp. 905–909, 2020, doi: 10.1109/LSP.2020.2998357.
- [5] P. Wang, J. Fang, X. Yuan, Z. Chen, and H. Li, "Intelligent reflecting surface-assisted millimeter wave communications: Joint active and passive precoding design," *IEEE Trans. Veh. Technol.*, vol. 69, no. 12, pp. 14960–14973, Dec. 2020.
- [6] P. Wang, J. Fang, L. Dai, and H. Li, "Joint transceiver and large intelligent surface design for massive MIMO mmwave systems," *IEEE Trans. Wireless Commun.*, vol. 20, no. 2, pp. 1052–1064, Feb. 2021.
- [7] X. Wang, Z. Fei, Z. Zheng, and J. Guo, "Joint waveform design and passive beamforming for RIS-assisted dual-functional radar-communication system," *IEEE Trans. Veh. Technol.*, vol. 70, no. 5, pp. 5131–5136, May 2021.
- [8] X. Wang, Z. Fei, J. Guo, Z. Zheng, and B. Li, "RIS-assisted spectrum sharing between MIMO radar and MU-MISO communication systems," *IEEE Wireless Commun. Lett.*, vol. 10, no. 3, pp. 594–598, Mar. 2021.
- [9] Z.-M. Jiang et al., "Intelligent reflecting surface aided dual-function radar and communication system," *IEEE Syst. J.*, early access, 2021, doi: 10.1109/JSYST.2021.3057400.
- [10] R. S. P. Sankar, B. Deepak, and S. P. Chepuri, "Joint communication and radar sensing with reconfigurable intelligent surfaces," in *Proc. IEEE 22nd Int. Workshop Signal Process. Adv. Wireless Commun. (SPAWC)*, 2021, pp. 471–475, doi: 10.1109/SPAWC51858.2021.9593143.
- [11] W. Lu, B. Deng, Q. Fang, X. Wen, and S. Peng, "Intelligent reflecting surface-enhanced target detection in MIMO radar," *IEEE Sens. Lett.*, vol. 5, no. 2, pp. 1–4, Feb. 2021.
- [12] W. Lu, Q. Lin, N. Song, Q. Fang, X. Hua, and B. Deng, "Target detection in intelligent reflecting surface aided distributed MIMO radar systems," *IEEE Sens. Lett.*, vol. 5, no. 3, pp. 1–4, Mar. 2021.

- [13] S. Buzzi, E. Grossi, M. Lops, and L. Venturino, "Radar target detection aided by reconfigurable intelligent surfaces," *IEEE Signal Process. Lett.*, vol. 28, pp. 1315–1319, 2021, doi: 10.1109/LSP.2021.3089085.
- [14] S. Buzzi, E. Grossi, M. Lops, and L. Venturino, "Foundations of MIMO radar detection aided by reconfigurable intelligent surfaces," 2021, arXiv:2105.09250v2.
- [15] K.-P.-H. Thai et al., "Detection-localization algorithms in the around-the-corner radar problem," *IEEE Trans. Aerosp. Electron. Syst.*, vol. 55, no. 6, pp. 2658–2673, Dec. 2019.
- [16] X. Guo, C. S. Ng, E. de Jong, and A. B. Smits, "Concept of distributed radar system for mini-UAV detection in dense urban environment," in *Proc. Int. Radar Conf. (RADAR)*, 2019, pp. 1–4.
- [17] A. Aubry, A. De Maio, and M. Rosamilia, "Reconfigurable intelligent surfaces for N-LOS radar surveillance," *IEEE Trans. Veh. Technol.*, vol. 70, no. 10, pp. 10735–10749, Oct. 2021.
- [18] V. Jamali, G. C. Alexandropoulos, R. Schober, and H. V. Poor, "Low-to-zero-overhead IRS reconfiguration: Decoupling illumination and channel estimation," 2021, arXiv:2111.09421v2.
- [19] E. Björnson, d. Özdogan, and E. G. Larsson, "Reconfigurable intelligent surfaces: Three myths and two critical questions," *IEEE Commun. Mag.*, vol. 58, no. 12, pp. 90–96, Dec. 2020.
- [20] M. A. Richards, Fundamentals of Radar Signal Processing. New York, NY, USA: McGraw-Hill, 2005.
- [21] M. Grant and S. Boyd, "CVX: Matlab software for disciplined convex programming, version 2.1," 2014. Accessed: 2021. [Online]. Available: http://cvxr.com/cvx
- [22] Z.-Q. Luo, W.-K. Ma, A. M.-C. So, Y. Ye, and S. Zhang, "Semidefinite relaxation of quadratic optimization problems," *IEEE Signal Process. Mag.*, vol. 27, no. 3, pp. 20–34, May 2010.
- [23] F. Wang and H. Li, "Joint waveform and receiver design for co-channel hybrid active-passive sensing with timing uncertainty," *IEEE Trans. Signal Process.*, vol. 68, pp. 466–477, 2020, doi: 10.1109/TSP.2020.2964194.
- [24] S. Boyd and L. Vandenberghe, Convex Optimization. Cambridge, U.K.: Cambridge Univ. Press, 2004.
- [25] O. E. Ayach, S. Rajagopal, S. Abu-Surra, Z. Pi, and R. W. Heath, "Spatially sparse precoding in millimeter wave MIMO systems," *IEEE Trans. Wireless Commun.*, vol. 13, no. 3, pp. 1499–1513, Mar. 2014.
- [26] M. R. Akdeniz et al., "Millimeter wave channel modeling and cellular capacity evaluation," *IEEE J. Sel. Areas Commun.*, vol. 32, no. 6, pp. 1164–1179, Jun. 2014.